Plasmonic Material Engineering for Targeted Therapeutics

Florentsen, Christoffer Dam; Moreno Pescador, Guillermo Sergio; Kjær, Andreas; Oddershede, Lene Broeng; Bendix, Poul Martin

Plasmonic Material Engineering for Targeted Therapeutics

Christoffer D. Florentsen, Guillermo S. Moreno-Pescador, Andreas Kjær,
Lene B. Oddershede,* and Poul Martin Bendix*

Nanomedicine approaches based on targeted delivery of nanoparticles have enormous therapeutic potential. For this to succeed, the nanoparticles, possibly functionalized or activatable by lasers, need to reach their target in the organism and preferably accumulate at this target. However, administration of nanoparticles in vivo results in rapid clearance of the particles by the immune system, thus preventing the nanomedicine in reaching its target. Passivation by polymer coatings has provided some success, but has not been sufficient to transform nanomedicine into an effective therapy. Recently, a new approach has been adopted which utilizes native cellular membranes for coating of nanoparticles. Motivated by the signaling and recognition capabilities of natural cell membranes, it is now feasible to produce nanoparticles with both immune evasive and tumor targeting abilities. Circulation times are dramatically enhanced by natural membrane coatings allowing significant increase in the passive accumulation by the enhanced permeability and retention effect. Membrane coating of nanoparticles provides a promising new development for advanced nanoparticle photothermal therapy (PTT). Here, the recent advances and challenges facing this new type of nanoparticle technology, bridging advanced optical properties with bio-compatibility, are reviewed with a focus on membrane coating of plasmonic nanoparticles which has shown great promise in PTT.

1. Introduction

Due to their advanced optical properties, plasmonic nanoparticles are receiving an increased interest for photothermal therapy (PTT). This is evident from the rise in number of publications in these two fields within the last two decades (**Figure 1**). One

C. D. Florentsen, Dr. G. S. Moreno-Pescador, Prof. L. B. Oddershede,
Prof. P. M. Bendix
Niels Bohr Institute
University of Copenhagen
Blegdamsvej 17, Copenhagen DK-2100, Denmark
E-mail: oddershede@nbi.ku.dk; bendix@nbi.ku.dk
Prof. A. Kjær
Department of Clinical Physiology, Nuclear Medicine & PET and Cluster
for Molecular Imaging
Department of Biomedical Sciences
Rigshospitalet & University of Copenhagen
Blegdamsvej 3, Copenhagen DK-2200, Denmark

key challenge, however, related to the use of nanoparticles for therapeutic purposes, is the lack of efficient methods to up-concentrate the particles at the site for therapeutic action, for example, in a tumor.[1] Upon successful targeting and up-concentration, much more efficient drugs could be used than if the nanoparticle loaded with drugs is distributed randomly throughout the entire organism. Also, lower dosages would be needed to achieve satisfactory levels of drugs at the desired site of delivery.[2] Furthermore, biopharmaceutical drugs such as enzymes, peptides, and antibodies are becoming more and more popular as therapeutic agents. However, biopharmaceuticals are large molecules (in the kDa range), which impose challenges in the delivery step due to low permeability through biological barrier interfaces such as cell membranes, mucus associated barriers, as well as the skin.[3]

These factors introduce a need for improved integration of drugs in delivery agents, targeting to specific action sites, and a means of cargo-release either through outer stimuli, for example, triggered by laser light, or by an encoded "unlock and release mechanism" that is activated at the appropriate location inside the organism.

Nanocarriers, for instance in the form of metallic nanoparticles, exhibit several attractive features such as easy functionalization with targeting molecules into tumors and can exhibit intrinsic physical properties like plasmonic absorption.[3,4] One of the key features to take advantage of using nanoparticles (NPs) is the enhanced permeability and retention (EPR) effect, which is a well-described phenomenon in cancer tissue, but also present in tissue with increased vascular permeability, for example, at sites of infection.[5] Nanoparticles with sizes larger than 10 nm are significantly larger than molecular drugs and are therefore not exposed to renal clearance and urinal excretion. Hence, certain size intervals of nanoparticles can extravasate through leaky vasculature, as often present in tumors, and hence the EPR effect effectively causes a localized delivery of drugs in the tumor, this is illustrated in **Figure 2**.[6] However, clinical trials have failed at exploiting the EPR effect successfully, making targeting ever so relevant.[7]

NPs can be either functionalized or engineered into having desirable features, that is, prolonging circulation time in the blood stream, incorporation of cargo molecules, or being activatable by lasers for a controlled release of drugs.[8–11]

Additionally, NPs such as FDA-approved poly(lactic-*co*-gly-colic acid) (PLGA) and poly(caprolactone) (PCL) particles are biodegradable and have been studied as drug cargo vehicles.[9]

Inorganic NPs, especially gold NPs (AuNPs), have a great potential due to several features: First, the ease of surface modification with biomolecules through thiol bonds allows for specific targeting without involving complex chemistry.[12,13] Second, the recent developments in inorganic NP synthesis allows for fabrication of a wide array of NPs with different sizes, shapes, and surface charge.[4,14,15] The variety in NP shapes which can be fabricated today opens up interesting applications within thermoplasmonics which relies on the plasmonic properties of AuNPs. Plasmonic heating produced by irradiation of metallic NPs makes them feasible as remotely controllable nanoheaters[16] for thermoplasmonic treatment,[4,17] imaging purposes, as well as vehicles for controlled release of cargo from the particle itself.[8,11,18] AuNPs are able to absorb the energy from a focused light source and convert it into a very localized heating.[15] The ability to tune the absorption spectrum of AuNPs is very promising in nanomedicinal treatments as the particles' absorbance of light can be shifted into the biological transparency window (BTW) which exists in the near-infrared (NIR) regime. This can be done by altering the shape, size, or composition of the NPs, thereby taking advantage of the light as a nearly noninvasive tool, which inflicts only little (possibly non-essential) damage on healthy tissue.[19]

These factors make plasmonic NPs promising candidates in the search for novel therapies of diseases such as cancer.[20] Considerable efforts have been made to design NP-based drug delivery systems for up-concentrating NPs at the desired therapeutic site. However, a careful review from 2016 going through 10 years of literature on this topic demonstrated that on average in literature, only 0.7% of the administered nanoparticles were found to be delivered at tumor sites and no "killer method" was reported.[1] Hence, upscaling from mice to human levels still poses a major challenge, and to this end, even more advanced NPs bridging optics and biology need to be developed.

2. Nanoparticles Relevant for Membrane Coating and PTT

Today, there is a vast array of commercially available NPs in a biocompatible quality to be used for nanomedicinal purposes; examples are discussed in **Figure 3**. The warehouse of NPs ranges from lipid based particles such as liposomes and micelles, polymeric particles, and polymer conjugates such as poly(ethylene glycol) (PEG)-based particles and PLGA encapsulating drugs to inorganic particles like AuNPs, and organic particles such as carbon nanotubes and dendrimers.[9,21–23] In the following, we devote our attention to plasmonic NPs and describe the characteristic optical properties of this class of particles and motivate their use as membrane camouflaged nanostructures.

2.1. Plasmonic Nanoparticles

The first known use of plasmonic NPs is in ancient art such as the Roman's Lycurgus cup from the fourth century, where

Christoffer Florentsen received his B.Sc. degree in nanoscience in 2013 and his M.Sc. degree in nanoscience in 2016 from the Niels Bohr Institute, University of Copenhagen, Copenhagen, Denmark. In 2017, he began his Ph.D. degree in experimental biophysics under the supervision of associate professor P. M. Bendix. His research interests include plasmonic heating of nanoparticles, dynamics of membranes, and proteins and nanoparticle delivered therapy.

Lene Broeng Oddershede is a professor of physics at the Niels Bohr Institute, University of Copenhagen, senior vice president at the Novo Nordisk Foundation, and a member of the Royal Danish Academy of Sciences and Letters. She has made significant contributions to the advancement of optical manipulation of nanoparticles and biological systems. Her research focuses on the interaction between light and nanoparticles and on unravelling biomechanical properties of molecules, cells, tissues, and organisms.

Poul Martin Bendix is an associate professor and group leader at the Niels Bohr Institute, University of Copenhagen. His main research interests include experimental biophysics including dynamics of cell surface structures and membrane proteins. He has contributed significantly to the understanding of thermoplasmonics of nanoparticles and the interactions between plasmonic nanoparticles and cell membranes.

the dichroism is evident from holding a light source inside or outside the cup. The reason for this phenomenon was found in 1990 to be due to the presence of metallic particles (66.2% silver, 31.2% gold, and 2.6% copper) in the nanometer range inside the glass.[24] The amazing colors found in the cup are due to scattering and absorption properties from the diverse metallic NPs in different size regimes.
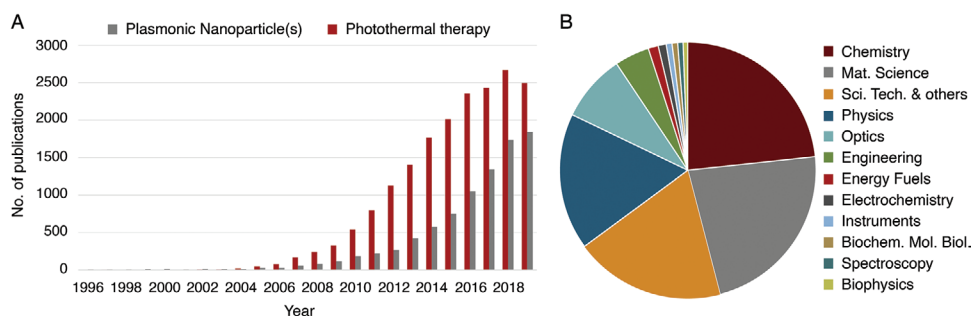
**ADVANCED
SCIENCE NEWS**

www.advancedsciencenews.com

**ADVANCED
OPTICAL
MATERIALS**

www.advopticalmat.de

Figure 1. A) Plot of number of publications within the topics "plasmonic nanoparticle(s)" and "photothermal therapy" showing the increase in scientific papers available from the Web of Science database in late March 2020. B) Research area-distribution of papers within the topic "plasmonic nanoparticles" pointing to the significance in fields such as physics, biophysics, and material science. Data show the 12 most prevalent research fields.

A key advantage of plasmonic NPs is that they can be activated by external laser light. Hence, it is possible to control NP heating and thereby PTT or release of cargo with high precision in time and space. The light-to-heat conversion by plasmonic nanoparticles, when irradiated by electromagnetic waves, peaks when resonant light optimally excites the electronic oscillations within the NP (Figure 3A); heat is generated from so called Joule heating,[25] which originates from friction between the electrons and the metallic lattice.

The interaction between light and a plasmonic NP will depend on the composition, size, and geometry of the NP and on its environment.[4,26] This interaction can be described through the extinction cross section (C_{ext}), which is defined as the sum of scattering and absorption cross sections. The extinction cross section of a particle embedded in a dielectric medium with permittivity ε_m and irradiated at a given wavelength λ can be described by the optical theorem[27]

$$C_{ext} = \kappa \, \text{Im}(\alpha) \tag{1}$$

where the wavenumber is $\kappa = 2\pi\sqrt{\varepsilon_m}/\lambda$ and α is the polarizability of the particle. When the size of the NP is much smaller than the wavelength, the scattering can be neglected and we get $C_{abs} \sim \kappa \text{Im}(\alpha)$. For small particle sizes, the polarizability is given by

$$\alpha = 3V \frac{\varepsilon(\omega) - \varepsilon_m}{\varepsilon(\omega) + \phi\varepsilon_m} \tag{2}$$

Here, V is the volume of the particle, ε is the dielectric permittivity of the particle at the given frequency ω, ε_m is the dielectric permittivity of the medium, and ϕ is a shape dependent parameter,[28] which for a sphere equals 2. The resonance is found when the absorption and scattering cross sections are at their maximum. The resonance wavelength is also dependent on the shape-dependent parameter, ϕ, and can be found as[29] $\lambda_{max} = \lambda_p \sqrt{\varepsilon_{ib} + \phi\varepsilon_m}$, where ε_{ib} is the electronic interband transition contribution and λ_p is the plasmon wavelength in the bulk material.

In practice, this means that light absorption and scattering can, through this mechanism, exhibit a fine sensitivity to small changes in the shape of a NP, as for instance when modulating the aspect ratio of gold nanorods[4,30] or varying the thickness of a gold layer in gold nanoshells (AuNSs)[4] (see Figure 3C). On the other hand, increasing the size of a spherical AuNP does not lead to a significant shift in the resonance, although there is a substantial increase of absorption with size as shown by the calculated result in Figure 3B.

The extreme size, composition, and shape-dependent characteristics of the optical absorption outlined above is a major reason for the significant attention devoted to plasmonic NPs in literature, as evident from Figure 1. It is of particular interest to tune the absorption to the NIR because this allows for external laser-induced activation of plasmonic NPs within living specimens for heat production with high precision in time and space without essential damage to the surrounding tissue.

2.1.1. Gold Nanoparticles

Among the huge variety of currently available plasmonic NPs, AuNPs have received much attention due to their low cytotoxicity and commercial availability in a reproducible and biocompatible quality and in a variety of sizes,[4,14] (see overview in Figure 3D).

Irradiation of gold nanoparticles has been extensively used in photothermal applications. The generation of heat originates from the absorption of optical energy, followed by a dissipation of heat into the medium surrounding the nanostructure.[31] Equilibration of the heat distribution in the surrounding medium is achieved within ≈ 100 ns[32] with the radial extension of the elevated thermal profile away from its surface being of the same magnitude as the size of the plasmonic particle.[33]
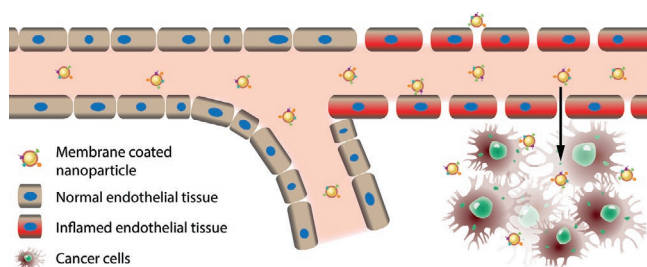

Figure 2. Schematic illustration of the enhanced permeability and retention effect. This effect helps up-concentration of drug-loaded nanoparticles of certain sizes by passive targeting. The effect is strongly enhanced by prolonged circulation times in the bloodstream, which can be achieved by various camouflage coatings.
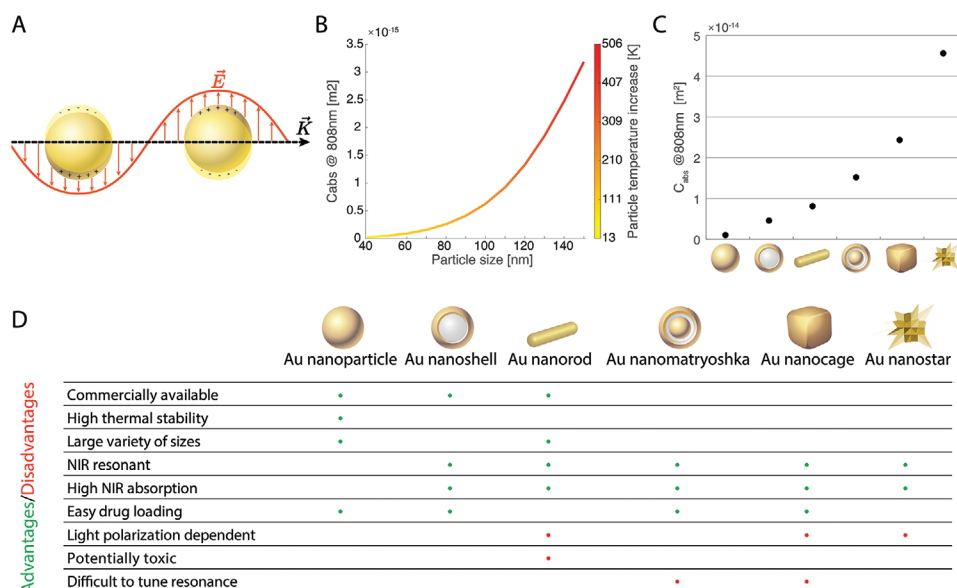
Figure 3. Plasmonic properties of metallic nanoparticles depend on their size and shape. A) Illustration of the interaction between the electric field from electromagnetic radiation and the conduction electrons in a metallic NP. B) The absorption cross section at $\lambda = 808$ nm as a function of particle diameter for a spherical and solid AuNP using an intensity of 9×10^6 W cm^{-2}. The temperature increase at the surface of the particle is visualized by the colorbar. C) Absorption coefficients for different types of irradiated NPs at $\lambda = 808$ nm: Spherical and solid AuNPs with d = 100 nm; AuNS with $d_{inner} = 80$ nm and $d_{shell} = 15$ nm; gold nano-rods (AuNRs) with length $l = 120$ nm and width $w = 30$ nm; gold nanomatryoshkas (AuNMs)[38] with $d_{inner} = 29$ nm, $d_{intermediate} = 10$ nm, and $d_{shell} = 13$ nm; gold nano-cubes (AuNCs)[39] with $l = 100$ nm, wall$_{thickness} = 10$ nm, and corner$_{holediameter} = 10$ nm; gold nanostars (AuNSt) with $d_{core} = 80$ nm, $l_{tip} = 25$ nm, and tip$_{diameter} = 5$ nm. Numbers are taken from Ref. [4]. D) Overview of advantages and disadvantages of a selection of gold nanoparticles relevant for photothemal therapy.

By solving the heat transfer equation,[34] the temperature increase in the vicinity of an irradiated NP can be calculated through the relation[16]

$$\Delta T(D) = \frac{R^3 I}{3DKV} C_{abs} \qquad (3)$$

Here, C_{abs} is the absorption cross section, mentioned above, which is defined as the ratio between the power absorbed by the particles and total incoming laser intensity (power per area). C_{abs} can be found using Mie theory. R is the radius of the particle, V is the particle volume, I is the intensity on the particle, D is the distance from the center of the particle, and K is the thermal conductivity of the medium in which the particle is suspended.

Using Equation (3), the heating of individual particles can be calculated. The temperature increase is directly proportional to C_{abs} and Figure 3B shows how C_{abs} depends on particle diameter for solid spherical AuNPs in water; the color code shows the NP's temperature increase if irradiated by a laser of wavelength of $\lambda = 808$ nm with a power density of 9×10^6 W cm^{-2}. Figure 3C shows how the absorption cross section of different NPs with resonance in the NIR depends on their shape and composition while irradiated with a laser of wavelength of $\lambda = 808$ nm. As suggested in ref. [17], the use of this specific wavelength allows for heating of AuNPs embedded within tissue while avoiding damage to the surrounding healthy tissue. We note that Equation (3) describes heating of a single nanoparticle; however, photothermal therapy is most often performed using particle concentrations exceeding 10^9 NPs mL^{-1};

under such conditions, collective heating effects from neighbouring NPs significantly alter the absorption,[35] hence, lower laser powers are needed to achieve a specific temperature than predicted by Equation (3).

Experimental measurements of heating from individual plasmonic nanoparticles have been carried out using nano-thermometry.[16,36] Such measurements allow for an experimental determination of C_{abs} by using Equation (3), whereby the optimal nanostructure for a photothermal application can be identified. It was observed that at a distance corresponding to the particle's radius away from the particle's surface, the temperature increase drops significantly (by $\approx 30-40\%$). This is important to take into consideration since collective effects giving rise to bulk heating can only be achieved when the heating distributions from individual nanoparticles have sufficient overlap.[35,37]

Due to the large diversity in commercially available plasmonic NPs, including AuNPs, AuNSs, nanomatryoshkas, nanostars, nanorods, and many more,[4] it is now possible to choose NPs with high absorption cross section at practically any wavelength. The summary in Figure 3D gives an overview of the different characteristics for several relevant plasmonic gold nanoparticles.

One of the key features of metallic NPs is the high surface-to-volume ratio. This allows for adding a high number of functionalization molecules to the particles per volume. The ease of functionalization of AuNPs, due to a favorable interaction between gold and the sulfur in thiols, has led to a multitude of added molecules such as various drugs,[40,41] miRNA[11] and siRNA,[18] DNA,[42] peptides,[43] and "stealth molecules"

**ADVANCED
SCIENCE NEWS**

www.advancedsciencenews.com

**ADVANCED
OPTICAL
MATERIALS**

www.advopticalmat.de

such as PEG molecules.[23] A challenge to consider if using metallic nanoparticles in vivo is the tendency to agglomerate when the particles are introduced into a saline solution due to the decrease in Debye length facilitated by the ions in solution.[13,44] Introduction into the blood stream will expose particles to a milieu containing salts, amino acids, enzymes etc., thus exposing the particles to a variety of destabilizing factors that may increase agglomeration. Agglomeration, however, will increase the local concentration of the particles which may be beneficial for reaching higher temperature upon laser irradiation due to collective effects.[35]

2.1.2. Other Nanoparticles

Several inorganic particles made from materials like Ag, Pt, Pd, Li, Na, Al, or other alternative plasmonic materials are currently being tested for their photothermal properties and do hold potential for future use with NIR light.[45–47]

Copper sulfide nanoparticles (CuSNPs) are known to exhibit a significant absorption in the NIR spectrum.[48] However, the reason for the absorption is not found in the plasmonic properties, but rather in energy band–band transitions. An increase in temperature was observed when an aqueous solution of CuSNPs was irradiated with a NIR laser (808 nm) over the course of 15 min.[48] In the same study, it was shown that cell viability decreased significantly after laser irradiation in HeLa cells. Furthermore, the cytotoxicity was investigated and compared to AuNPs and $CuCl_2$, indicating a lower cytotoxic effect from the CuSNPs. The small drawback on the CuSNPs is the inability to tune the absorbance peak. Hence, the peak is located at ≈900 nm for all sizes, but it is evident that the absorption power increases with particle size.

In recent years, iron-oxide nanoparticles (ION)s such as Fe_3O_4 have received much attention in fields ranging from biomedicine and healthcare to energy, agriculture, and construction.[49] The obvious advantage of using IONs in biomedicine as an alternative to AuNPs is their low production costs and their magnetic properties. Furthermore, the dual functionality of the particles (i.e., magnetic properties along with plasmonic properties) makes these particles a versatile tool in both imaging and PTT. Hence, they can be used as contrast agents with magnetic resonance imaging (MRI), and using an alternating magnetic field, heat can be generated, which can be utilized for hyperthermia as well as drug delivery. Furthermore, the particles are biocompatible due to the fact that iron is a nutrient metabolized in the body.[49,50] Recently, the photothermal properties of IONs have been given more attention.[51–53] Although the plasmonic properties of IONs are not as pronounced as their gold counterpart, they have been shown to increase the temperature of their surroundings following treatment with an NIR (808 nm) laser.[51] The plasmonic properties of IONs were further studied by Shen et al.,[52] who showed that the interaction with light is greatly enhanced when the particles cluster together. It was found that the absorption of the clustered particles was significantly higher than the single particle assay and a 3.6-fold increase in the absorption at 808 nm was found. Furthermore, cell viability was affected by the clustering of particles, following NIR laser irradiation, and cell death was more pronounced for the clustered particles. The use of IONs in PTT is complicated by the fact that particles tend to aggregate in saline solutions which might increase the photothermal effect in the biological transparency window, but might reduce accumulation by the EPR effect (see Figure 2), due to the large size of the aggregates. Clustering of the Fe_3O_4 NPs is also expected to happen once they have been administered in vivo and should be resolved by using efficient coatings.

One drawback of using inorganic NPs in vivo is the potential problem of upconcentration in vital organs such as the liver and spleen[54] (see also Figure 6). To overcome this challenge, biomembrane-coated polymeric nanoparticles have been explored for drug delivery purposes. However, as these particles do no exhibit the optical or magnetic properties needed for PTT and special imaging purposes (i.e., MRI), these particle types are not covered here in detail and we recommend refs. [55–67] to the interested reader.

3. Membrane Coating of Plasmonic Nanoparticles

Most bio-incompatible NPs are recognized by the immune system as foreign objects and hence become excreted from the blood stream within a few hours and accumulate in the liver and spleen. Therefore, there is a need for a stealth or biomimicking approach which will be essential for having the particles circulating in the bloodstream long enough for a significant amount to reach the desired destination.

For many years, functionalization with PEG molecules (PEGylation) has been the state-of-the-art method for prolonging NP circulation time in the body, thus facilitating passive targeting.[2,3] PEGylation of particles forms a hydrated polymeric brush layer which neatly prevents protein adsorption and opsonization.[68] Furthermore, PEGylation lowers the uptake-rate by the organs (liver and spleen), has low intrinsic toxicity, and is soluble in water, which also increase drug solubility in water. To further solidify the importance of PEG in biological applications, the resulting steric hindrance contributes to a lowering of any charge-induced interactions with the body or other particles due to a decrease of zeta-potentials.[69] The "stealth" properties of PEGylation has been well established and several PEG-coated particles are already FDA approved or in clinical trials.[69–71] As an example, coating of AuNPs with PEG molecules has been shown to prolong circulation time in rats where 18% of the AuNPs was still found circulating in the blood after 24 h (compared to 0.1% for particles coated with the colloidal stability enhancing molecule bis(p-sulfonatophenyl)phenylphosphine).[72]

Even though PEGylation of particles has been used for decades, the polymer has proved to have some flaws. For example, PEG derivatives have been investigated with respect to two different cell lines where the findings suggest a moderate cytotoxicity for certain PEG derivatives when introduced to mouse fibroblasts (L929).[73] Other studies have found that anti-PEG antibodies are expressed in some healthy individuals[74] and PEG has a tendency to induce blood clotting due to non-specific interactions between blood and PEG polymers. Also, PEG-containing liposomes have been found to be able to induce hyper-sensitivity reactions which might provoke

an anaphylactic shock in a worst case scenario. For a thorough review on PEGylation, we encourage the reader to read ref. [69].

Several polymeric alternatives to PEG have been proposed, many of which show the same efficacy as PEG.[23] Polyvinylpyrrolidone (PVP) and polyoxazolines (POX) are two types of polymers that have been tested as alternatives to PEG. For example, AuNPs have been coated with oligo(2-ethyl-2-oxazoline), a POX polymer which can be modified to bind to a specific particle surface.[75] Furthermore, a peptide sequence was added for recognition of a specific $\beta 1$ integrin, overexpressed in A549 lung cancer cells. These POX-coated AuNPs are promising, especially for cancer imaging purposes. PVP has been used to functionalize AuNPs along with doxorubicin (DOX) for A549 lung cancer cell apoptosis,[76] and addition of PVP to IONs showed low cytotoxicity and low aggregation in water and was used as an MRI contrast agent.[77] It should be noted, however, that PVP has been reported to have trouble with biodegradability and immunogenicity.[78] Several other polymeric stealth coatings have been proposed, for example, polyglycerols, polyacrylamides, polyaminoacids, and polysaccharides.

Although PEG and other types of polymers have provided significant progress to the delivery part of NPs, there is an urgent need to find new strategies to further increase circulation times with preferentially biomimetic and nontoxic materials. An interesting approach is to exploit nature's own fabrication of interfaces, namely the cellular plasma membrane, which we review in the following section.

3.1. Biomembrane Mimicking

In recent years, biomimetic approaches to prolonging the circulation of nanotherapeutics have been suggested. These include coating different types of NPs with cell-derived membranes like red blood cells (RBC),[55,79] white blood cells (WBC),[62,80] cancer cells,[81] stem cells,[82,83] or blood platelets[79] as well as functionalization with well known "do-not-eat-me"-signal activating molecules like CD47.[68,84] This concept is schematically illustrated in **Figure 4**, where nanoparticles are coated with different types of cell membranes followed by injection into the bloodstream and subsequent up-concentration in the tumor. Furthermore, membranes from bacteria have been studied as a coat and could potentially help in the development of antibacterial vaccines when used as a coating of AuNPs.[85] The motivation for using membrane coating to camouflage NPs is summarized in **Figure 5**, which shows a promising and improved delivery and therapeutic effect of a number of different types of membrane-coated NPs tested in vivo.

In the following section, we focus on the coating of plasmonic NPs using mammalian cell types for treatment of diseases such as cancer as well as for enhancing imaging conditions. NP coatings by plasma membranes from different cell types are outlined and the specific advantages and disadvantages associated with the respective cell type are discussed. Also, there are descriptions of the different methods used for extracting cellular plasma membranes and discussion of subsequent coating strategies.
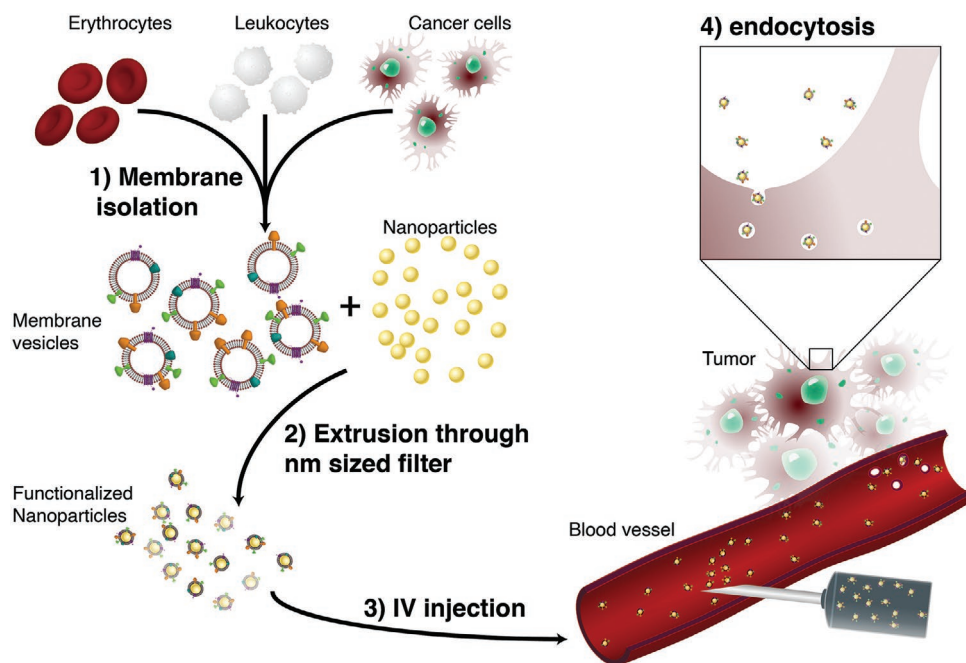

Figure 4. Schematic showing the sequence of membrane coating, particle injection, EPR, and endocytosis into tumor cells. 1) Membranes from cells of interest are isolated through various methods. 2) The isolated membranes are then mixed with the NPs and extruded through a nanometer sized filter in order to facilitate functionalization and membrane coating of the particles. Validation of successful membrane coating can be performed using various techniques like dynamic light scattering or transmission electron microscopy to detect size changes caused by addition of a coating. 3) Intravenous injection of the functionalized and membrane-coated particles facilitate high concentrations and prolonged circulation in the bloodstream. 4) Endocytosis into tumor cells facilitated by the EPR effect.
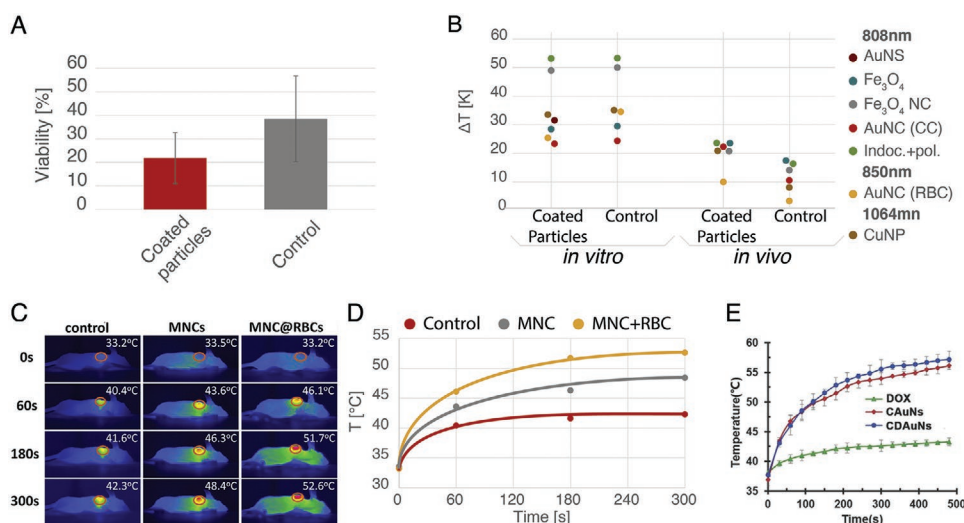
Figure 5. Overview of viability and temperature increase after laser irradiation of membrane-coated NPs (or non-coated control NPs) inside tumor cells and inside mice inoculated with tumors. Data are taken and summarized from refs. [67,86–90] (ref. [91] is a part of the in vitro "coated particles" data; however, it only contains data from WBC-coated particles, but no control data). A) Viability of tumor cells obtained from six different studies based on laser treatment of tumor cells cultured with membrane coated plasmonic NPs (in the controls, the NPs were not membrane coated). Both the control and the coated particles were treated with NIR laser. It should be noted that one study uses PVP coated particles as a control[86] and that another study uses DOX without particles as control.[87] From the same study, the herein reported data demonstrate the viability of cells containing only coated nanocages, that is, without DOX. As a control for the CuNPs reported in ref. [90], NIR laser and DOX were used without particles. For the indocyanine + polymer study, a soy lecithin membrane was used for the control particles.[67] In summary, the data demonstrate that the viability of tumors containing coated nanoparticles is lower than the controls without. B) Temperature increase for different types of irradiated plasmonic NPs used for PTT. The type of NIR laser used in each study is stated above each particle type with the indicated wavelengths. Interestingly, the temperature increase in vivo is overall higher for the membrane-coated NPs. C) Images taken with a temperature-sensitive camera during PTT in mice using Fe_3O_4 nanoclusters. Reproduced with permission.[89] Copyright 2016, Elsevier. The effect of membrane coating of the NPs is substantial compared to the controls. D) Quantification of the temperature data from experiments shown in (C). The fits are arbitrary and only have the purpose of visualizing the asymptotic tendency of the heating. Data are reproduced with permission from Ren et al.[89] The in vivo data shows a sharp increase followed by an asymptotic behavior and a clear positive effect of the membrane coating. E) Temperature increase in tumor tissue of mice using AuNCs. Reproduced with permission.[87] Copyright 2017, Wiley-VCH. Here, green dots signify the control without membrane coating; also in this experiment, membrane coating gives a clear positive effect on temperature increase.

3.1.1. Erythrocytes

Of all of the cell types used as membrane donors for NP functionalization, the RBCs, also known as erythrocytes, are the most widely used. Mature RBCs do not contain a cell nucleus and lack internal organelles. Furthermore, the RBCs are naturally able to remain in the bloodstream for ≈120 days and the membrane contains several "markers of self," which inhibits immune activation responses.[92–94] Hence, RBCs make up a complex biological system that can be utilized for membrane donation for further functionalization of desired NPs, and they are abundantly present in a normal blood sample. Ghosts, a term describing the discoid bodies of RBCs after removal of hemoglobin, have been known since the 1960s[95] and the protocol has been further developed to be used for functionalization of NPs.[55]

The use of plasmonic NPs for functionalization with cell membranes was first reported in 2013 by Gao et al.[96] Here, AuNPs were used as carriers of RBC membranes. The ghosts from RBCs were extruded through 100 nm filters in a suspension with dispersed AuNPs to facilitate the fusion of membrane and particles. The functionalization was confirmed by transmission electron microscopy (TEM) as well as dynamic light scattering (DLS). Furthermore, the NPs were able to interact with antibodies that are known to recognize the RBC exoplasmic protein

CD47, thus confirming the functionalization of the RBC coating. To investigate the effect of the membrane coating on the stealth properties of the NPs, macrophage uptake was monitored after 30 min of incubation with J774 murine macrophages, showing a significantly larger uptake of uncoated AuNPs.

Piao and Wang et al.[86] demonstrated that coating with RBC membranes prolongs the circulation time in mice compared to particles covered in a poly(vinylpyrrolidone) (PVP) coating, which has been proposed as a potential alternative to PEG.[69] They coated gold nano-cages (AuNCs) with RBC membrane and introduced the particles in mice for evaluation.[86] The particles retained the hollow core as well as porous structure, as confirmed by TEM. Furthermore, the particles did not change their plasmonic properties and no alterations of the UV–vis spectrum was observed after coating. The stealth properties of the membranes were shown by a lower amount of particles taken up by cells as well as by the biodistribution which suggested that the particles accumulate more at the tumor site and less in the major organs compared to PVP coated particles (see **Figure 6**).

In an effort to take advantage of the plasmonic properties of AuNPs, Ahn et al. utilized AuNPs for X-ray imaging of the RBCs in the bloodstream.[98] Here, instead of coating the NPs with membranes, the AuNPs were incorporated into RBCs to be used as a contrast agent with X-ray imaging. By incubating the RBCs with AuNPs with different surface-chemistry under
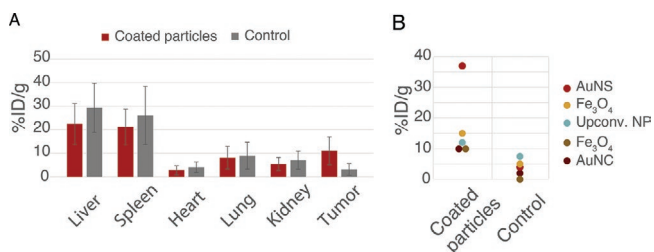
ADVANCED
SCIENCE NEWS
www.advancedsciencenews.com

ADVANCED
OPTICAL
MATERIALS
www.advopticalmat.de

Figure 6. Overview of NP biodistribution and retention time in organs of mice using membrane coated NPs as well as un-coated control NPs. The biodistribution data are from refs. [67,86–91,97]. The retention time data are take from refs. [86,88,89,91,97]. A) Biodistribution of membrane-coated NPs (red) and of control NPs (gray) 48 h after injection. This summary of biodistribution is based on seven studies involving photo-activatable NPs. One of these studies uses PVP coating for controls both in vivo and in vitro.[86] Another study uses coated AuNS with DOX loading where the control is coated AuNS without DOX.[87] B) Retention in the bloodstream after 24 h. The retention in the blood is measured as %ID g^{-1}. The plot is based on five different studies of membrane-coated plasmonic NPs. One of these studies uses PVP-coated particles as a control.[86]

hypotonic conditions, the RBCs incorporated the particles, thus potentially enabling dynamic X-ray imaging of blood flow.

A combination of RBC and platelet membranes was used to create biomimetic NPs for biodetoxification and removal of pathogenic bacteria.[99] Due to the diverse interactions of bacteria and their subsequent hemolytic toxins with the human body, a NP bearing a multitude of biological functions was prepared from gold nanowires and the two different types of membrane.

The use of IONs in biomedicine has increased in recent years due to the large range of opportunities in biomedical applications.[100] In an attempt to create a biomimetic NP for combined MRI and PTT, Ren et al.[89] used magnetic nanoclusters which had already been shown to produce significant heating during laser irradiation at 808 nm.[52] The RBC-coated IONs showed an increased retention in the blood as well as improved cytotoxicity after laser irradiation in MCF-7 cancer cells. The biodistribution of the coated IONs were studied and showed an increased tumor accumulation as well as a lower percentage of particles localized in the spleen, liver, and kidney compared to bare IONs (see Figure 6). Furthermore, they were able to show a positive result after irradiation of tumors in mice. Here, it was found that the tumor growth was inhibited after laser irradiation of the coated NPs compared to mice without laser irradiation.

Another promising biomimetic nanoparticle was prepared by Rao et al.[88] By taking advantage of electroporation to create multiple membrane pores that small molecules and NPs can flow through, they were able to make a coating of RBC membrane on the surface of IONs. The coated particles showed a significantly improved colloidal stability compared to bare IONs, indicating a surface functionalization that enhances stability, which is attributed to the hydrophilic glycans on the RBC surface. Following introduction of the particles to MCF-7 cancer cells, it was obvious that the cytotoxic effect was significant after laser irradiation with an 808 nm laser. Furthermore, the particles showed an increased blood retention as well as an ability to decrease tumor growth in mice.

As mentioned earlier, CuSNPs are capable of turning light into heat through the absorption of light at 900 nm.[48] It has been shown that CuSNPs can be coated with a hybrid membrane of RBC membranes and cancer cell membranes (melanoma B16-F10 cells).[90] The particles showed an improved retention in the blood of mice indicating an effect from the membrane coating as well as an increased uptake in tumor tissue compared to bare NPs. For PTT, the NPs were incubated with B16-F10 cells and irradiated with a 1064 nm laser. This treatment showed a high cytotoxic effect compared to treatments without the particles, and even treatment with DOX proved to be less effective than the PTT. The tumor repression was studied in mice, showing that the tumor progression was inhibited significantly when CuSNPs were irradiated with a 1064 nm laser.

3.1.2. Leukocytes

WBCs, also known as leukocytes, are an interesting cell type to utilize as donor for NP coating. WBCs are a vital part of the human organism and the cells of the immune system. The cells are able to identify and eliminate pathogens and foreign substances in the body, thus being part of the primary defense system. Furthermore, WBCs are part of the repair process of damaged tissue.

WBC-coated particles were first reported in a study where three different types of leukocytes membranes (J774 macrophages, THP-1 monocytes, and Jurkat T lymphocytes) were coated onto 2.8 µm silica particles containing nanopores by Parodi et al.[62] The coating of such particles significantly lowered the particle internalization compared with naked particles, especially when the investigated cell type matched the membrane coating. The membrane-coated particles were able to specifically bind to inflamed HUVEC endothelial cells due to a distribution of lymphocyte function-associated antigen 1 (LFA-1) on the particles, which facilitated recognition of the LFA-1 receptor, ICAM-1, on the HUVEC cells. Furthermore, WBC membrane coated particles, loaded with DOX, were able to transport the drug through an endothelial cell layer and lower the viability of MDA-MB-231 cancer cells on the other side of the layer.

The use of WBC-coated NPs was further developed in 2017 by Kang et al.[60] Neutrophils, which are the most abundant type of erythrocyte in the human body, were here used as donors for PLGA NPs. The coated particles showed a preference for the pre-metastatic site mimicked by HUVEC cells activated by TNF-α, with an almost threefold increase in NPs in the TNF-α activated cells compared to non-treated cells. Inactivation of the LFA-1 receptor, ICAM-1, showed a significant decrease in associated particles, indicating that ICAM-1 signaling plays an important role in recruiting WBC membranes, and thus in recruitment of coated NPs. Furthermore, the WBC membrane coated NPs were introduced in a lung metastatic mouse model and demonstrated a better correlation between the coated NPs compared to the uncoated particles.

The publication by Xuan et al.[91] is, to our knowledge, the only report containing data on plasmonic NPs coated with leukocyte membranes. A coating on gold nanoshells (AuNS)s with

**ADVANCED
SCIENCE NEWS**
www.advancedsciencenews.com

**ADVANCED
OPTICAL
MATERIALS**
www.advopticalmat.de

macrophage membrane using the extrusion method showed a coating of the membrane on the particle, confirmed by a 14 nm increase in particle size, measured with DLS. Using flow cytometry, it was shown that an internalization of particles in 4T1 cancer cells was almost two times higher than when using bare NPs. Furthermore, the circulation time in mice increased and the accumulation at the tumor site increased. As a last test, mice were intravenously injected in the tail with AuNSs covered with WBC membranes followed by laser irradiation at 808 nm (1 W cm^{-2}) for 5 min. The results showed a clear decrease of tumor growth, as opposed to an increase in all control groups. The possibilities with an assay taking advantage of the finely tuneable plasmonic properties of such particles and the clear targeting advantages of leukocyte membranes toward tumor cites can be of great importance for the future of PTT in cancer patients.

3.1.3. Cancer Cells

Cancer cell membranes have been given much attention due to the obvious importance of targeting cancer cells and the possibility of homotopic targeting.[65–67,87,90,97] PTT in cancer treatment has without a doubt received considerable attention through the last decades, owing to the targeting possibilities, the EPR effect, and the fact that a highly localized treatment is achievable. Several polymeric NPs have been coated with cell membranes from cancerous tissue,[65,66] and much effort has gone into functionalizing plasmonic particles with cancer cell membranes, copper NPs,[90] AuNCs,[87] and a plasmonic polymer.[67]

The photothermal properties of indocyanine green (ICG) was utilized for PTT by Chen et al.[67] By incorporating ICG into polymeric cores, NPs with plasmonic properties were obtained. The particles were functionalized with the membranes of MCF-7 cancer cells using standard coating method (detailed below) but in the presence of a PEG lipid (PEG-DSPE), the result being a polymeric plasmonic NP with a cancer cell cloak. The temperature increase following laser treatment was confirmed using infrared thermal imaging. The NPs showed a preference for MCF-7 cancer cells compared to other types of cancer and non-cancer cells. To evaluate the PTT possibilities, tumor-bearing mice treated with NPs were followed for 18 days without visible relapse of the tumor as opposed to the control.

Sun et al. developed a multi-step mechanism for cancer therapy using AuNCs.[87] The first step involved incorporation of DOX for biochemical treatment of cancer and the second step was the coating of the AuNCs with membranes from 4T1 cancer cells to target the tumor site. The AuNCs could then be used as drug carriers followed by PTT using a NIR laser. The results without laser treatment showed a lower cell viability when using DOX-loaded particles than pure DOX, which might be due to an increased uptake of membrane-coated particles by the cells. The viability dropped to almost zero as laser was applied, indicating that the PTT effect in combination with a high concentration of DOX was highly efficient for cancer treatment in vitro. In vivo studies further showed a significant decrease in tumor volume as the combination of DOX and PTT was used compared to either method alone.

In an effort to accommodate the need for in vivo highly specific tumor imaging methods, Rao et al. constructed a particle based on up-conversion nanoprobes.[97] Up-conversion nanoprobes are capable of converting NIR light to light in the visible region.[101] This, combined with a low cytotoxicity and the membrane coating possibilities, makes the probes very interesting as imaging agents for cancer visualization. Vesicles derived from cancer cells by hypotonic treatment were mixed with the AuNCs followed by extrusion. The particles obtained showed an increased size and confirmation of a 9.8 nm membrane coat was shown using TEM. Imaging of the particles showed an increased signal at the tumor site, especially when using a membrane cloak equal to the type of tumor.

The specificity in targeting, as well as the promising results from combining drug loading and PTT, makes cancer cells a promising candidate for membrane coating donors and subsequent targeting and treatment.

3.1.4. Mesenchymal Stem Cells

The surface of mesenchymal stem cells (MSCs) expresses a multitude of receptors that can bind to tumor expressed ligands. This natural tumor homing ability can be exploited for drug delivery by using the stem cell membranes for coating NPs. MSCs additionally have a natural ability to evade the immune system which is a property expected to be inherited by the MSC membrane coated NPs. Furman et al.[83] demonstrated the efficiency of nanoghosts derived from MSC membranes for efficient targeting both in an in vitro and an in vivo system. The nanoghosts were additionally loaded with doxorubicin and led to an 80% inhibition of prostate cancer. Also, nanogels have been successfully coated with MSC membranes providing the NPs with tumor targeting ability and prolonging their circulation time in vivo.[82] The hypo-immunogenicity combined with targeting property makes MSCs membranes highly attractive as a coating material in nanomedicine, but has yet to be thoroughly investigated for camouflaging plasmonic NPs.

3.2. Methods for Membrane Isolation and NP Coating

The coating of NPs using cell membranes involves membrane isolation by various methods. The quality of the plasma membrane coating is imperative for establishing an efficient biointerface between the NP and immune cells, and hence the coating strategy needs attention to ensure functionality of the membrane and its embedded membrane proteins.

The coating strategy should ideally preserve the state of the native membrane, including all the protein parts which may constitute up to 50% fraction of the membrane area.[102] The complex mixture of lipids and proteins contained in the plasma membrane is apparently much more efficient in evading the immune system than simple lipid mixtures which have been used in liposome formulations for drug delivery during the last decade. This clearly shows that careful extraction of the plasma membrane from cells and proper NP coating are critical steps for achieving successful particles for drug delivery.
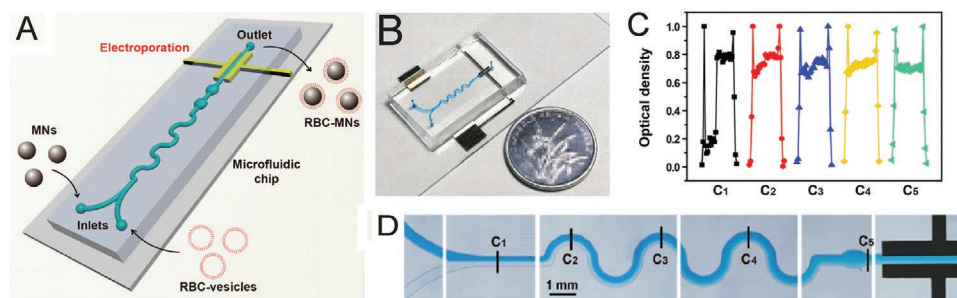
Figure 7. A microfluidic electroporation assay for efficient coating of nanoparticles with RBC membranes. A) Schematic showing the device consisting of an S-formed microfluidic channel with an electroporation device at the end of the channel. The combined microfluidic and electroporation device facilitates nanoparticle cloaking with RBC membranes by adding the vesicles and nanoparticles in two different inlets followed by thorough mixing in the S-shaped channel. The electroporation zone ensures pore formation in the RBCs which the nanoparticles can go through. B) Demonstration of the relative scale of the device. C) Calibration of the mixing efficiency of the two inlets as a function of time. D) Images from mixing of pure water with water containing a blue dye showing progressive mixing along the S-shaped channel. Reproduced with permission.[88] Copyright 2017, American Chemical Society.

As indicated in the previous section, the coating of NPs by membranes can be performed by several methods and these rely on physical and biochemical steps and depend on the type of cell used as a membrane donor.

Red blood cells are the simplest type of cells and can be hypotonically swollen and directly mixed with NPs, and by extrusion it is possible to achieve membrane coating.[2] The isolation of RBC-membrane-derived vesicles involves centrifugation followed by hypotonic treatment for hemolysis followed by another centrifugation step to remove the hemoglobin to produce so-called ghosts.[55] This rather simple protocol makes it feasible for utilizing the RBC vesicles for NP camouflage for significantly prolonging the circulation time in the body.

In ref. [88], the coating of magnetically active NPs by red blood cell membranes was improved by using a microfluidic device to mix NPs with hypotonically swollen red blood cells (see **Figure 7**). The RBC vesicles were mixed with IONS in a microfluidic chip followed by applying a pulsating electrical field, which facilitated the merging of IONs and RBC membranes (see Figure 7).

Coating of NPs by membranes from more complex cell types like stem cells, cancer cells, or immune cells requires isolation of the cell membrane from other organelles prior to coating. This can be done by disruption of cells by hypotonic treatment followed by sonication and ultracentrifugation to facilitate isolation of the membrane part, which then becomes a homogenized mass of lipids and membrane proteins.[83] Similar to the coating procedure with RBC membranes, the isolated membrane mass can be extruded together with the NPs through narrow filters with slightly larger holes than the size of the NPs to be coated. This process has been proven to yield a membrane layer on the NP, as shown by TEM images of stem cell membrane coated NPs[82] or macrophage-coated NPs[91] (see **Figure 8**).

The flexibility of the coating procedure of NPs is also demonstrated by approaches which combine membranes from different cell types to form a hybrid coating on NPs. The RBC membrane can be fused to membranes from other cell types followed by coating of the NPs with the fused mixture. This approach was used in ref. [90], where RBC membranes were isolated for further use and B16-F10 cell membranes were extracted using a membrane protein extraction kit. The two membranes were fused by sonication and the fusion was confirmed by Förster resonance energy transfer (FRET) between the mixed donor and acceptor fluorophores originating from the two membranes. The particle coating was simply achieved by sonication of a mixture of CuSNPs and RBC-B16 membranes.

3.3. Membrane Leaflet Orientation

The plasma membrane of cells contains highly organized and oriented proteins and a lipid asymmetry with most of the negatively charged lipids residing on the inner leaflet. A loss of the natural membrane asymmetry can have functional implications if the membrane-coated NPs are supposed to mimic a natural membrane and hence avoid early clearance from the blood stream. Additionally, if homotypic targeting is used for, for example, cancer cell membranes, only receptors with the proper orientation will participate in recognition of specific moieties on the cancer cells. Orientation of the membrane cloak is therefore an important aspect to consider when coating NPs.

Characterization of the membrane coating remains poorly studied and most often the focus is on verifying that a membrane layer of ≈10 nm thickness is in fact present on the NP surface, thus indicating successful membrane coating (see Figure 8). The crude isolation method for separating the lipid material from a cell, and the subsequent extrusion process, could result in a random orientation of the proteins within the plasma membrane coating. Further studies are needed to resolve the actual protein orientation within the NP coating and to assess the quality of the lipid bilayer, which could be filled with nanoscopic defects. Such studies would have the potential to further improve the effectiveness of membrane coatings in the targeting of NPs. Intriguingly, despite this lack of characterization, most studies report an impressive targeting efficiency and long circulation times when NPs are coated with material from cellular plasma membranes,[82,83,91] thus indicating that membrane coating may constitute a robust stealth coating approach regardless of protein orientation. However, this could be optimized and a significant improvement of the aforementioned properties could be harvested.
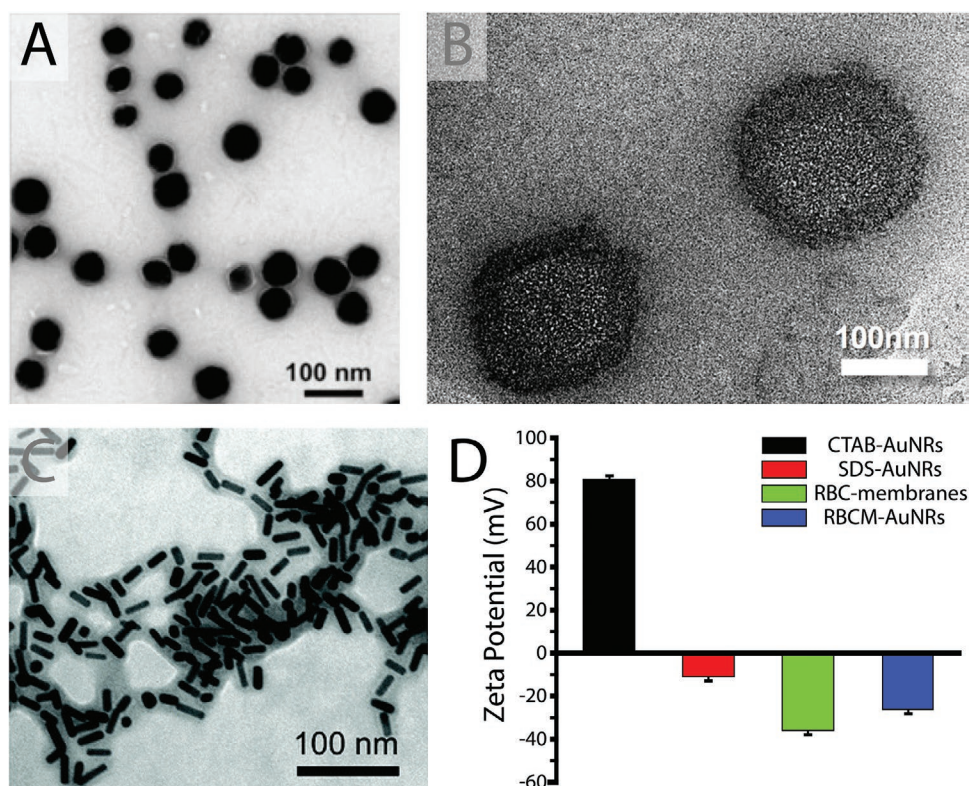
Figure 8. Characterization of membrane coating after coating of nanoparticles using red blood cell (RBC) membranes or plasma membranes isolated from cancer cells. A) Transmission electron microscopy (TEM) image of gold nanoparticles with a membrane cloak from RBCs. Reproduced with permission.[96] Copyright 2013, Wiley-VCH. B) TEM image of polymeric indocyanine green loaded nanoparticles coated with a cell membrane from MCF-7 cancer cells. Reproduced with permission. [67] Copyright 2016, American Chemical Society. C) TEM image of gold nanorods (AuNRs) coated with RBC membranes. D) Zeta potential measured for AuNRs with different types of surfactant coatings (CTAB: cetyl trimethyl ammonium bromide, SDS: sodium dodecyl sulfate, RBCM: red blood cell membrane) compared with zeta potential of intact RBC membranes. (C,D) Reproduced with permission.[103] Copyright 2018, Royal Society of Chemistry.

3.4. Giant Plasma Membrane Vesicles

Another strategy for isolating membranes has been to trigger vesiculation of cells, thus forming giant plasma membrane vesicles (GPMVs).[104,105] The GPMVs have been shown to contain the plasma membrane proteins from the donor cell with a correct orientation. Future work should exploit that these vesicles mimic the plasma membrane closely and experiments should be performed to see whether NP coating works by extruding or sonicating such vesicles in presence of NPs. It will be interesting to see if the resulting membrane coating obtained by this method differs from the methods described above. The orientation of membrane proteins can be tested by proteases which cleave off specific parts of the proteins which reside on the outer side of the membrane and hence are accessible to enzymes.[104]

Not all NPs may be suitable for membrane coating. Successful coating of a bilayer membrane necessitates a hydrophilic NP surface to allow for a thin hydration layer between the metal and the headgroups of the inner membrane leaflet. Coating of metallic NPs with a polymer cushion would ideally provide a water layer between the metal surface and the membrane, thus facilitating fluidity of the membrane. Coating of flat surfaces like glass coverslips or mica surfaces with both artificial membranes and cellular plasma membranes is a well

established technique.[106] This results in fluid membranes with a minor interaction with the substrate, which can be further minimized by tethering the bilayer to the substrate with either polymers[107] or other novel tethering strategies.[108] Whether a similar strategy is feasible for coating of NPs remains to be explored.

3.5. Characterization Issues

There is a huge lack of methods to characterize the biophysical state of the coating membranes. Most studies rely on TEM imaging and DLS measurements to verify a diameter increase consistent with a membrane thickness. TEM imaging provides detailed information on the thickness of the electron-dense part of the NP coating. The lipid bilayer of cells is known to have a thickness of ≈5–6 nm and with an additional protein cloak, a somewhat thicker coating of 10 nm as detected by TEM imaging.[67,96,103] Drawbacks of using TEM imaging for characterizing the NP coating include poor statistics due to single particle based quantification and, more importantly, the necessary dehydration of the sample may affect the membrane.

Dynamic light scattering allows for detection of the hydrodynamic diameter of NPs before and after coating in an

**ADVANCED
SCIENCE NEWS**
www.advancedsciencenews.com

**ADVANCED
OPTICAL
MATERIALS**
www.advopticalmat.de

aqueous environment, in contrast to TEM. The hydrodynamic diameter includes the particle, the protein coat, and possible additional polymeric extensions. Polymers extending from the membrane may be invisible by TEM, but contribute to the DLS-measured diameter, which is based on diffusional properties of the particle.

Molecular packing of the membrane layer can be measured using environmentally sensitive probes like Laurdan or C-Laurdan, which both measure the extent of water penetration into the membrane.[105,109] Laurdan molecules intercalate between the lipids and the probe exhibits a red-shift upon contact with water molecules. Hence, a red-shift of the Laurdan emission spectrum indicates a membrane with a more fluid character and thereby reports about the physical state of the membrane. Finally, calorimetry can be used to identify the actual transition temperature of both artificial and natural membranes.[110]

A physical characterization of membrane coating, which is possible using Laurdan probes or calorimetry, has so far not been applied to membrane coating of plasmonic nanoparticles. Future efforts should be made to compare the fluidity of NP coatings with cellular membranes. Notably, the extreme curvature exhibited by the NP surface and the adhesion to the surface may cause changes in the membrane as indicated by some studies.[111,112]

The orientation of the proteins embedded within the membrane coating should also be assessed. This could, for example, be assessed by using proteases which can cleave off the protein part containing, for example, a fused green fluorescent protein (GFP).[104] The degree of loss of GFP signal indicates the fraction of proteins oriented toward the outer side of the membrane.

Other challenges in membrane coating assays include complete removal of nucleic matter since genetic safety is essential when injecting material from cancer cells and stem cells into the blood stream. Such concerns can be alleviated by treating with RNases and DNases, thus preventing induction of malignancies. Finally, upscaling and standardization of protocols will be critical for transition from lab bench to bedside for the benefit of patients.

As a guide to the reader, we summarize in **Table 1** the reported coatings of various NPs, including plasmonic and magnetic NPs, with associated references. Furthermore, the most significant advantages and disadvantages are listed in **Table 2**. The types of NPs explored with membrane coatings are rapidly expanding and the overview provided in Table 1 and 2 does not provide a complete list of references.

4. Current and Future Challenges

If proper coating of NPs by intact plasma membranes can be achieved, we envision this technology has tremendous potential to be used for both hiding the NPs from the immune system while also providing efficient targeting. Clever approaches can combine the stealth technology provided by natural and biomimetic membranes with genetic approaches to induce expression of specific cancer antigens or receptors. By genetically modifying donor cells to express both membrane receptors

Table 1. Overview of cell membrane coated nanoparticles of different types.

Cell type	Particle type	Ref.
RBC	Polymeric*	[55–58]
	AuNPs†	[96]
	AuNPs‖†	[98]
	Au nanocages†	[86]
	Au nanorods†	[103]
	Fe$_3$O$_4$ NP‡†	[88]
	Fe$_3$O$_4$ nanoclusters‡†	[89]
	Melanin†	[114]
RBC and platelets	Au nanowires†	[99]
RBC and cancer cells	Copper sulfide nanoparticles†	[90]
WBC	Polymeric*	[59–62]
	Au nanoshells†	[91]
Platelets	Polymeric*	[63]
Epithelial cells	Polymeric*	[64]
Cancer cells	Au nanocages†	[87]
	Indocyanine green + polymer†	[67]
	Upconversion nanoprobes^b	[97]
	Polymeric*	[65, 66]
Myeloid-derived suppressor cells	Fe$_3$O$_4$ NP‡†	[115]
Bacteria	AuNPs†	[85]

RBC, red blood cells; WBC, white blood cells. The *symbol indicates PLGA, PLA, etc. The †symbol indicates plasmonic particles. The ‡symbol indicates Fe$_3$O$_4$, which has previously been shown to redshift the resonance peak of AuNP, if they are used as a coating.[113] The ^{b}symbol indicates fluorescent nanoprobes capable of converting NIR light to visible light[101] and finally, the ‖symbol indicates incorporation of the particle into cells.

which can target cancer cells and proteins which convey a non-threatening signal to the immune system, it will be possible to design very attractive membrane coated NPs for future drug delivery and for delivering functional plasmonic NPs for PTT. Harvesting intact plasma membranes from cells overexpressing either peripherally binding annexin proteins or transmembrane viral proteins has been demonstrated recently,[104] which should be extended to cells expressing relevant proteins for efficient targeting such as CD47.

Coating of NPs using other natural membranes like exosomes also provides efficient passivation of NPs in vivo.[116] Exosomes are small vesicles around 100–1000 nm in diameter which are secreted from most cell lines and can easily be harvested by collecting the culturing medium containing the secreted vesicles. Exosome-coated NPs were recently prepared by a one-step method simply by sonication of the NP/exosome mixture.[116] Exosomes are naturally involved in cell–cell signaling, and exosome membranes may therefore be very interesting in terms of targeting NPs to specific tissues.

4.1. Future of Plasmonic Nanostructures

The thermoplasmonic properties of nanostructures have been extensively investigated and it is now possible to identify optical

Table 2. Overview of advantages and disadvantages of each type of membrane coating mentioned in Table 1.

		Cell Type						
		RBC	WBC	Platelets	Epithelial cells	Cancer cells	Mds. cells	Bacteria
Advantages/ **Disadvantages**	Natural expression of ''do-not-eat-me signal''	•						
	Prolongued blood retention	•	•			•	•	
	Reduced macrophage uptake	•	•					
	Nuclei-free cells	•		•				
	Abundant volumes in the blood	•	•	•				
	Active targeting		•	•	•	•	•	
	Facilitates homotypic targeting					•		
	Immune activation							•
	Upscaling particle coating	•	•	•	•	•	•	•
	Standardization of particle coating	•	•	•	•	•	•	•

RBC, red blood cells; WBC, white blood cells; Mds. cells, myeloid-derived supressor cells.

nanostructures for specific applications.[4] Some of the most efficient NIR absorbers include shells, rods, cubes, and stars made of gold. Also, other alternative materials exhibit high absorption in the NIR region as discussed in this review. As a guide to the reader, advantages and disadvantages of promising nanostructures are listed in Figure 3D. All structures listed in Figure 3D are made from gold; gold is an attractive material because it is bio-compatible, non-toxic, and well suited for chemical conjugation. The structures with resonances that can be tuned into the NIR are especially attractive; the gold nanorod (AuNR) is an example of an NP with a high NIR absorption, a well-established chemical synthesis, commercial availability, and a favorable surface-to-volume ratio for drug conjugation. We envision that this nanostructure combined with camouflaging membrane-based strategies, as reviewed here, is an interesting candidate for future theranostic applications involving PTT.

However, plasmonic nanostructures also possess other attractive features when combined with thermoresponsive materials. Combining their efficient light-to-heat conversion with thermoresponsive membrane coatings adds another functionality to drug release controlled by irradiation.[117] For instance, gold nanostructures are well known to induce phase transitions and associated leakage in artificial membranes upon irradiation[36,118,119] and this property can be exploited in membrane-coated nanostructures. Gold nanocubes (AuNCs) are particularly interesting candidates in this context since they can be designed to exhibit NIR resonance and their hollow interior allows encapsulation of drugs. Combined with a thermoresponsive membrane coat with incorporated immuno-evasive peptides or proteins, AuNCs offer significant possibilities for tomorrow's therapies.

4.2. Alternative Coatings

As described earlier, PEGylation has long been the preferred functionalization method of NPs for prolonging circulation time in the bloodstream. Using an approved standard chemical like PEG is desirable with respect to translation into clinical settings and in terms of commercial upscaling of NP production. However, due to several problems arising from using this type of molecule,[69,73,74] a search for proteins involved with evading macrophage uptake has been of great importance. Future efforts should therefore uncover which components within the natural membrane are critical for the significant increase in circulation times observed for NPs coated with natural membranes. The integrin-associated protein, CD47, has a broad spectrum of functions as a cell surface receptor.[68] Of great importance, however, is the "do-no-eat-me" signal that it is able to pass on to macrophages upon binding to the signal-regulatory protein α on the macrophage membrane. The binding triggers a protein-binding cascade, resulting in inhibition of the Fcγ receptor-dependent endocytosis by macrophages.[68,84] It is known that a functionalization method involving CD47 will help polystyrene particles evade phagocytosis by certain macrophages, thus prolonging circulation in the bloodstream.[84] Recently, a peptide derived from CD47 was incorporated into artificial liposomes and resulted in significant inhibition of macrophage uptake[120] (see **Figure 9**).

One favorable approach of protein functionalization of biomimetic NPs is thus to facilitate evasion by identifying critical components of biological membranes, such as CD47, and incorporate these into the composition of a synthetic cloak used for coating plasmonic NPs. Furthermore, using synthetic lipids for the membrane coat can provide a future direction for industry-scale production of membrane-coated NPs with purified components from, for example, membranes from red blood cells, thus recapitulating the properties of the natural membranes. This could overcome the bottleneck of upscaling the production of native cell membranes and the inherent difficulty in standardizing and commercializing the production of membrane coats derived from living cells.

4.3. Effect of the Protein Corona

It is important to note that introduction of foreign objects, such as AuNPs, to the human body will cause a reaction. One of the very important aspects of this is the protein
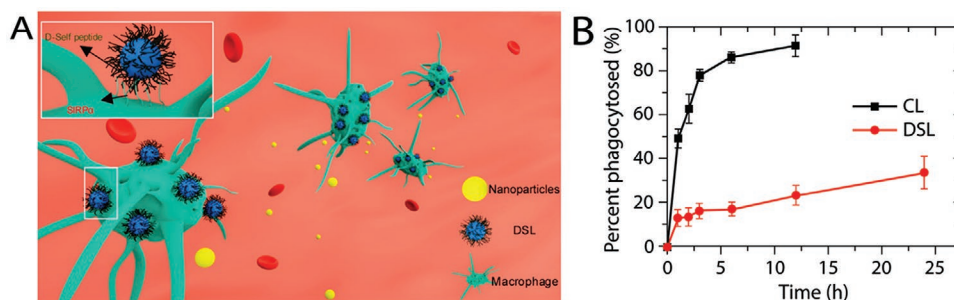
ADVANCED
SCIENCE NEWS
www.advancedsciencenews.com

ADVANCED
OPTICAL
MATERIALS
www.advopticalmat.de

Figure 9. A liposome-based bio-inspired nanoparticle containing a CD47-derived peptide (D-self-peptide) on the surface. A) The peptide conveys a do-not-eat-me signal to macrophages, thus preventing initiation of phagocytosis. B) Uptake of conventional liposomes and D-self-peptide-labeled liposomes as a function of time, showing a dramatic inhibition of uptake caused by the peptide. Reproduced with permission.[120] Copyright 2019, American Chemical Society.

corona formation on the surface of NPs introduced to the blood. NPs administered in vivo spontaneously and within minutes, acquire a protein corona, which consists of a complex protein coat from blood components. This also applies to NPs coated with natural membranes and the effect of a protein corona on macrophage uptake should be investigated. Several factors affect the formation of a corona, such as milieu, NP features (i.e., size, shape, and charge as well as functionalization by molecules/membrane), and conditions such as temperature, incubation period, and the timescale that the particles are circulating in the bloodstream.[121] Hadjidemetriou et al. found that the composition of proteins in the corona fluctuated over time and that the total amount of protein on the surface was more or less constant, indicating a competitive nature of corona formation inside the bloodstream.[78] Interestingly, the protein adsorption on leukosomes, which are bio-mimetic nanovesicles derived from leukocytes, were found to form less extensive protein corona compared to artificial liposomes, thus confirming the advantages of nature's own recipe for making bio-interfaces.[121] It is therefore important to be extra careful when drawing conclusions from in vitro experiments on NP uptake in cell cultures, since in vitro NPs are not exposed to the protein adsorption that occurs in the bloodstream, the flow changes, and possibly small changes in pH which are factors that may affect NP–cell interactions.

Finally, the effect of the membrane coating on the plasmonic properties of nanoparticles should be characterized. There is, however, evidence suggesting that membrane coatings, or other biological coatings, do not affect the plasmonic characteristics of NPs significantly. Cancer cell membrane coated AuNSs and ICG-polymeric core particles did not show any significant difference in the bulk light absorption capabilities.[67,87] Similar results were found for a variety of different RBC-coated nanoparticles[88–90,114] and macrophage-coated AuNSs.[91] This is not surprising since the membrane, or other types of organic material, correspond to adding a very thin layer of dielectric material to the NP and will therefore not change the C_{abs}. Biological material interacts poorly with the NIR wavelengths used in PTT,[122] and hence the plasmonic nanoparticles are expected to have a nearly identical plasmonic performance after addition of any type of biological coating. At lower wavelengths where absorption in biological material is higher, the membrane material could possibly interfere more with C_{abs}.[67,88]

4.4. Conclusion

The use of membrane-coated plasmonic nanoparticles is still in its infancy, but is quite promising due to the recently demonstrated significant improvements in circulation time, biodistribution, and therapeutic effect seen for a range of NPs coated
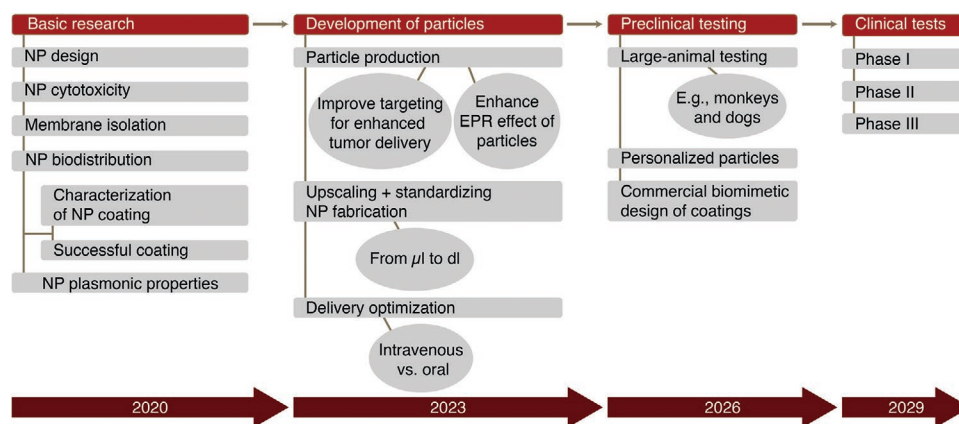

Figure 10. Proposed progress in the field of membrane-functionalized plasmonic nanoparticles for targeted photothermal therapy.

**ADVANCED
SCIENCE NEWS**

www.advancedsciencenews.com

**ADVANCED
OPTICAL
MATERIALS**

www.advopticalmat.de

with cell membranes from various cell types. We envision a productive line of development as depicted in **Figure 10** over the next decade with improved standardization and upscaling methods for synthesizing efficient membrane-coated plasmonic and polymeric nanoparticles. Metallic and especially AuNPs exhibit a great potential in biomedical applications when combined with cell membrane camouflaging as discussed in this review. It is important to mention that PTT using plasmonic nanoparticles can favorably be combined with other modes of interventions like immune-checkpoint inhibition,[123] which allows additional treatment of distant tumors. Importantly, the transition to clinical applications of plasmonic nanoparticles has already been demonstrated, as the first nanothermometry-based clinical study in humans has proved that AuNSs are able to ablate prostate cancer tumors with low re-occurrence after 12 months.[124] Also, the use of artificial biomimicking membranes as coating of NPs will be a leap forward as it will facilitate production and upscaling as well as provide a uniform and reproducible high quality basis for clinical applications and commercialization. We foresee that if production of membrane-coated nanoparticles can be upscaled, many successful clinical trials will be within reach in the near future.

Conflict of Interest

The authors declare no conflict of interest.

[1] S. Wilhelm, A. J. Tavares, Q. Dai, S. Ohta, J. Audet, H. F. Dvorak, W. C. W. Chan, *Nat. Rev. Mater.* **2016**, *1*, 16014.

[2] B. T. Luk, L. Zhang, *J. Controlled Release* **2015**, *220*, 600.

[3] S. Mitragotri, P. A. Burke, R. Langer, *Nature Rev. Drug Discov.* **2014**, *13*, 655.

[4] L. Jauffred, A. Samadi, H. Klingberg, P. M. Bendix, L. B. Oddershede, *Chem. Rev.* **2019**, *119*, 8087.

[5] E. A. Azzopardi, E. L. Ferguson, D. W. Thomas, *J. Antimicrob. Chemother.* **2013**, *68*, 257.

[6] H. Maeda, J. Wu, T. Sawa, Y. Matsumura, K. Hori, *J. Controlled Release* **2000**, *65*, 271.

[7] F. Danhier, *J. Controlled Release* **2016**, *244*, 108.

[8] R. Huschka, J. Zuloaga, M. W. Knight, L. V. Brown, P. Nordlander, N. J. Halas, *J. Am. Chem. Soc.* **2011**, *133*, 12247.

[9] R. Li, Y. He, S. Zhang, J. Qin, J. Wang, *Acta Pharm. Sin. B* **2018**, *8*, 14.

[10] D. E. Large, J. R. Soucy, J. Hebert, D. T. Auguste, *Adv. Ther.* **2018**, *2*, 1800091.

[11] C. D. Florentsen, A. K. V. West, H. M. D. Danielsen, S. Semsey, P. M. Bendix, L. B. Oddershede, *Langmuir* **2018**, *34*, 14891.

[12] V. Biju, *Chem. Soc. Rev.* **2014**, *43*, 744.

[13] R. M. Fratila, S. G. Mitchell, P. Del Pino, V. Grazu, J. M. De La Fuente, *Langmuir* **2014**, *30*, 15057.

[14] L. A. Dykman, N. G. Khlebtsov, *Chem. Rev.* **2014**, *114*, 1258.

[15] A. Samadi, L. Jauffred, H. Klingberg, P. M. Bendix, L. B. Oddershede, *Complex Light and Optical Forces XIII*, Proc. SPIE Vol. *10935*, SPIE, Bellingham, WA **2019**, pp. 94–103.

[16] P. M. Bendix, S. N. S. Reihani, L. B. Oddershede, *ACS Nano* **2010**, *4*, 2256.

[17] J. T. Jørgensen, K. Nørregaard, P. Tian, P. M. Bendix, A. Kjær, L. B. Oddershede, *Sci. Rep.* **2016**, *6*, 30076.

[18] R. Huschka, A. Barhoumi, Q. Liu, J. a. Roth, L. Ji, N. J. Halas, *ACS Nano* **2012**, *6*, 7681.

[19] L. A. Sordillo, Y. Pu, S. Pratavieira, Y. Budansky, R. R. Alfano, *J. Biomed. Opt.* **2014**, *19*, 056004.

[20] E. Hemmer, A. Benayas, F. Légaré, F. Vetrone, *Nanoscale Horiz.* **2016**, *1*, 168.

[21] D. Peer, J. M. Karp, S. Hong, O. C. Farokhzad, R. Margalit, R. Langer, *Nat. Nanotechnol.* **2007**, *2*, 751.

[22] A. Sangtani, O. K. Nag, L. D. Field, J. C. Breger, J. B. Delehanty, *Wiley Interdiscip. Rev.: Nanomed. Nanobiotechnol.* **2017**, *9*, e1466.

[23] N. Hadjesfandiari, A. Parambath, *Engineering of Biomaterials for Drug Delivery Systems*, Woodhead Publishing, Sawston, Cambridge **2018**, pp. 345–361.

[24] M. Loos, *Carbon Nanotube Reinforced Composites*, Elsevier, Amsterdam **2014**.

[25] G. Baffou, *Thermoplasmonics: Heating Metal Nanoparticles Using Light*, Cambridge University Press, Cambridge **2017**.

[26] E. Petryayeva, U. J. Krull, *Anal. Chim. Acta* **2011**, *706*, 8.

[27] C. F. Bohren, D. R. Huffman, *Absorption and Scattering of Light by Small Particles*, Wiley-VCH, Weinheim **1998**.

[28] N. G. Khlebtsov, L. A. Dykman, *J. Quant. Spectrosc. Radiat. Transf.* **2010**, *111*, 1.

[29] N. G. Khlebtsov, *Quantum Electron.* **2008**, *38*, 504.

[30] X. Huang, M. A. El-Sayed, *J. Adv. Res.* **2010**, *1*, 13.

[31] J. A. Webb, R. Bardhan, *Nanoscale* **2014**, *6*, 2502.

[32] Z. Qin, J. C. Bischof, *Chem. Soc. Rev.* **2012**, *41*, 1191.

[33] H. Ma, P. Tian, J. Pello, P. M. Bendix, L. B. Oddershede, *Nano Lett.* **2014**, *14*, 612.

[34] A. O. Govorov, W. Zhang, T. Skeini, H. Richardson, J. Lee, N. A. Kotov, *Nanoscale Res. Lett.* **2006**, *1*, 84.

[35] G. Baffou, P. Berto, E. B. Ureña, R. Quidant, S. Monneret, J. Polleux, H. Rigneault, *ACS Nano* **2013**, *7*, 6478.

[36] A. Kyrsting, P. M. Bendix, D. G. Stamou, L. B. Oddershede, *Nano Lett.* **2011**, *11*, 888.

[37] P. Keblinski, D. Cahill, A. Bodapati, C. Sullivan, T. Taton, *J. Appl. Phys.* **2006**, *100*, 054305.

[38] C. Ayala-Orozco, C. Urban, M. W. Knight, A. S. Urban, O. Neumann, S. W. Bishnoi, S. Mukherjee, A. M. Goodman, H. Charron, T. Mitchell, M. Shea, R. Roy, S. Nanda, R. Schiff, N. J. Halas, A. Joshi, *ACS Nano* **2014**, *8*, 6372.

[39] S. E. Skrabalak, J. Chen, Y. Sun, X. Lu, L. Au, C. M. Cobley, Y. Xia, *Acc. Chem. Res.* **2008**, *41*, 1587.

[40] F. Wang, Y. C. Wang, S. Dou, M. H. Xiong, T. M. Sun, J. Wang, *ACS Nano* **2011**, *5*, 3679.

**ADVANCED
SCIENCE NEWS**
www.advancedsciencenews.com

**ADVANCED
OPTICAL
MATERIALS**
www.advopticalmat.de

[41] B. Saha, J. Bhattacharya, A. Mukherjee, A. Ghosh, C. Santra, A. K. Dasgupta, P. Karmakar, *Nanoscale Res. Lett.* **2007**, *2*, 614.

[42] X. Zhang, M. R. Servos, J. Liu, *J. Am. Chem. Soc.* **2012**, *134*, 7266.

[43] J. Zong, S. L. Cobb, N. R. Cameron, *Biomater. Sci.* **2017**, *5*, 872.

[44] R. Pamies, J. G. H. Cifre, V. F. Espin, M. Collado-Gonzalez, F. G. D. Banos, J. G. De La Torre, *J. Nanopart. Res.* **2014**, *16*, 2376.

[45] G. V. Naik, V. M. Shalaev, A. Boltasseva, *Adv. Mater.* **2013**, *25*, 3264.

[46] G. H. Chan, J. Zhao, E. M. Hicks, G. C. Schatz, R. P. Van Duyne, *Nano Lett.* **2007**, *7*, 1947.

[47] A. Samadi, H. Klingberg, L. Jauffred, A. Kjaer, P. M. Bendix, L. B. Oddershede, *Nanoscale* **2018**, *19*, 9097.

[48] Y. Li, W. Lu, Q. Huang, C. Li, W. Chen, *Nanomedicine* **2010**, *5*, 1161.

[49] A. Ali, H. Zafar, M. Zia, I. ul Haq, A. R. Phull, J. S. Ali, A. Hussain, *Nanotechnol., Sci. Appl.* **2016**, *9*, 49.

[50] J. Estelrich, M. Busquets, *Molecules* **2018**, *23*, 1567.

[51] M. Chu, Y. Shao, J. Peng, X. Dai, H. Li, Q. Wu, D. Shi, *Biomaterials* **2013**, *34*, 4078.

[52] S. Shen, S. Wang, R. Zheng, X. Zhu, X. Jiang, D. Fu, W. Yang, *Biomaterials* **2015**, *39*, 67.

[53] P. Purohit, A. Samadi, P. M. Bendix, J. Laserna, L. B. Oddershede, *Sci. Rep.* **2020**, *10*, 1198.

[54] K. Nørregaard, J. T. Jørgensen, M. Simón, F. Melander, L. K. Kristensen, P. M. Bendix, T. L. Andresen, L. B. Oddershede, A. Kjær, *PLoS One* **2017**, *12*, e0177997.

[55] C. M. J. Hu, L. Zhang, S. Aryal, C. Cheung, R. H. Fang, L. Zhang, *Proc. Natl. Acad. Sci. USA* **2011**, *108*, 10980.

[56] C. M. J. Hu, R. H. Fang, B. T. Luk, K. N. H. Chen, C. Carpenter, W. Gao, K. Zhang, L. Zhang, *Nanoscale* **2013**, *5*, 2664.

[57] S. Aryal, C. M. J. Hu, R. H. Fang, D. Dehaini, C. Carpenter, D. E. Zhang, L. Zhang, *Nanomedicine* **2013**, *8*, 1271.

[58] J. Koo, T. Escajadillo, L. Zhang, V. Nizetz, S. M. Lawrence, *Frontiers in Pediatrics* **2019**, *7*, 410.

[59] Q. Zhang, D. Dehaini, Y. Zhang, J. Zhou, X. Chen, L. Zhang, R. H. Fang, W. Gao, L. Zhang, *Nat. Nanotechnol.* **2018**, *13*, 1182.

[60] T. Kang, Q. Zhu, D. Wei, J. Feng, J. Yao, T. Jiang, Q. Song, X. Wei, H. Chen, X. Gao, J. Chen, *ACS Nano* **2017**, *11*, 1397.

[61] X. Wei, G. Zhang, D. Ran, N. Krishnan, R. H. Fang, W. Gao, S. A. Spector, L. Zhang, *Adv. Mater.* **2018**, *30*, 1802233.

[62] A. Parodi, N. Quattrocchi, A. L. van de Ven, C. Chiappini, M. Evangelopoulos, J. O. Martinez, B. S. Brown, S. Z. Khaled, I. K. Yazdi, M. V. Enzo, L. Isenhart, M. Ferrari, E. Tasciotti, *Nat. Nanotechnol.* **2013**, *8*, 61.

[63] X. Wei, M. Ying, D. Dehaini, Y. Su, A. V. Kroll, J. Zhou, W. Gao, R. H. Fang, S. Chien, L. Zhang, *ACS Nano* **2018**, *12*, 109.

[64] P. Angsantikul, S. Thamphiwatana, Q. Zhang, K. Spiekermann, J. Zhuang, R. H. Fang, W. Gao, M. Obonyo, L. Zhang, *Adv. Ther.* **2018**, *1*, 1800016.

[65] R. H. Fang, C. M. J. Hu, B. T. Luk, W. Gao, J. A. Copp, Y. Tai, D. E. O'Connor, L. Zhang, *Nano Lett.* **2014**, *14*, 2181.

[66] H. Sun, J. Su, Q. Meng, Q. Yin, L. Chen, W. Gu, P. Zhang, Z. Zhang, H. Yu, S. Wang, Y. Li, *Adv. Mater.* **2016**, *28*, 9581.

[67] Z. Chen, P. Zhao, Z. Luo, M. Zheng, H. Tian, P. Gong, G. Gao, H. Pan, L. Liu, A. Ma, H. Cui, Y. Ma, L. Cai, *ACS Nano* **2016**, *10*, 10049.

[68] S. M. G. Hayat, V. Bianconi, M. Pirro, A. Sahebkar, *Int. J. Pharmaceutics* **2019**, *569*, 118628.

[69] K. Knop, R. Hoogenboom, D. Fischer, U. S. Schubert, *Angew. Chem. Int. Ed.* **2010**, *49*, 6288.

[70] P. Mishra, B. Nayak, R. K. Dey, *Asian J. Pharm. Sci.* **2016**, *11*, 337.

[71] C. M. J. Hu, R. H. Fang, B. T. Luk, L. Zhang, *Nanoscale* **2014**, *6*, 65.

[72] J. Lipka, M. Semmler-Behnke, R. A. Sperling, A. Wenk, S. Takenaka, C. Schleh, T. Kissel, W. J. Parak, W. G. Kreyling, *Biomaterials* **2010**, *31*, 6574.

[73] G. Liu, Y. Li, L. Yang, Y. Wei, X. Wang, Z. Wang, L. Tao, *RSC Adv.* **2017**, *7*, 18252.

[74] C. Lubich, P. Allacher, M. de la Rosa, A. Bauer, T. Prenninger, F. M. Horling, J. Siekmann, J. Oldenburg, F. Scheiflinger, B. M. Reipert, *Pharm. Res.* **2016**, *33*, 2239.

[75] a. S. Silva, M. C. Silva, S. P. Miguel, V. D. B. Bonifácio, I. J. Correia, A. Aguiar-Ricardo, *RSC Adv.* **2016**, *6*, 33631.

[76] V. Ramalingam, K. Varunkumar, V. Ravikumar, R. Rajaram, *Sci. Rep.* **2018**, 1.

[77] H. Y. Lee, N. H. Lim, J. A. Seo, S. H. Yuk, B. K. Kwak, G. Khang, H. B. Lee, S. H. Cho, *J. Biomed. Mater. Res. B, Appl. Biomater.* **2006**, *79*, 142.

[78] M. Hadjidemetriou, Z. Al-Ahmady, K. Kostarelos, *Nanoscale* **2016**, *8*, 6948.

[79] D. Dehaini, X. Wei, R. H. Fang, S. Masson, P. Angsantikul, B. T. Luk, Y. Zhang, M. Ying, Y. Jiang, A. V. Kroll, W. Gao, L. Zhang, *Adv. Mater.* **2017**, *29*, 1606209.

[80] W. He, J. Frueh, Z. Wu, Q. He, *Langmuir* **2016**, *32*, 3637.

[81] R. H. Fang, C. M. J. Hu, B. T. Luk, W. Gao, J. A. Copp, Y. Tai, D. E. O'Connor, L. Zhang, *Nano Lett.* **2014**, *14*, 2181.

[82] C. Gao, Z. Lin, B. Jurado-Sánchez, X. Lin, Z. h. Wu, Q. He, *Small* **2016**, *12*, 4056.

[83] N. E. T. Furman, Y. Lupu-Haber, T. Bronshtein, L. Kaneti, N. Letko, E. Weinstein, L. Baruch, M. Machluf, *Nano Lett.* **2012**, *13*, 3248.

[84] Y. Qie, H. Yuan, C. A. von Roemeling, Y. Chen, X. Liu, K. D. Shih, J. A. Knight, H. W. Tun, R. E. Wharen, W. Jiang, B. Y. S. Kim, *Sci. Rep.* **2016**, *6*, 1.

[85] W. Gao, R. H. Fang, S. Thamphiwatana, B. T. Luk, J. Li, P. Angsantikul, Q. Zhang, C. M. J. Hu, L. Zhang, *Nano Lett.* **2015**, *15*, 1403.

[86] J. G. Piao, L. Wang, F. Gao, Y. Z. You, Y. Xiong, L. Yang, *ACS Nano* **2014**, *8*, 10414.

[87] H. Sun, J. Su, Q. Meng, Q. Yin, L. Chen, W. Gu, Z. Zhang, H. Yu, P. Zhang, S. Wang, Y. Li, *Adv. Funct. Mater.* **2017**, *27*, 1910230.

[88] L. Rao, B. Cai, L. L. Bu, Q. Q. Liao, S. S. Guo, X. Z. Zhao, W. F. Dong, W. Liu, *ACS Nano* **2017**, *11*, 3496.

[89] X. Ren, R. Zheng, X. Fang, X. Wang, X. Zhang, W. Yang, X. Sha, *Biomaterials* **2016**, *92*, 13.

[90] D. Wang, H. Dong, M. Li, Y. Cao, F. Yang, K. Zhang, W. Dai, C. Wang, X. Zhang, *ACS Nano* **2018**, *12*, 5241.

[91] M. Xuan, J. Shao, L. Dai, J. Li, Q. He, *ACS Appl. Mater. Interfaces* **2016**, *8*, 9610.

[92] P. A. Oldenborg, A. Zheleznyak, Y. F. Fang, C. F. Lagenaur, H. D. Gresham, F. P. Lindberg, *Science* **2000**, *288*, 2051.

[93] C. M. J. Hu, R. H. Fang, L. Zhang, *Adv. Healthcare Mater.* **2012**, *1*, 537.

[94] J. W. Yoo, D. J. Irvine, D. E. Discher, S. Mitragotri, *Nature Rev. Drug Discovery* **2011**, *10*, 521.

[95] J. T. Dodge, C. Mitchell, D. J. Hanahan, *Arch. Biochem. Biophys.* **1963**, *100*, 119.

[96] W. Gao, C. M. J. Hu, R. H. Fang, B. T. Luk, J. Su, L. Zhang, *Adv. Mater.* **2013**, *25*, 3549.

[97] L. Rao, L. L. Bu, B. Cai, J. H. Xu, A. Li, W. F. Zhang, Z. J. Sun, S. S. Guo, W. Liu, T. H. Wang, X. Z. Zhao, *Adv. Mater.* **2016**, *28*, 3460.

[98] S. Ahn, S. Y. Jung, E. Seo, S. J. Lee, *Biomaterials* **2011**, *32*, 7191.

[99] B. E. F. de Ávila, P. Angsantikul, D. E. Ramírez-Herrera, F. Soto, H. Teymourian, D. Dehaini, Y. Chen, L. Zhang, J. Wang, *Science Robotics* **2018**, *3*, eaat0485.

[100] M. O. Ansari, M. F. Ahmad, N. Parveen, S. Ahmad, S. Jameel, G. G. H. A. Shadab, *Mater. Focus* **2017**, *6*, 269.

[101] G. Chen, H. Qiu, P. N. Prasad, X. Chen, *Chem. Rev.* **2014**, *114*, 5161.

[102] S. Takamori, M. Holt, K. Stenius, E. A. Lemke, M. Grønborg, D. Riedel, H. Urlaub, S. Schenck, B. Brugger, P. Ringler, S. A. Muller, B. Rammner, F. Grater, J. S. Hub, B. L. De Groot, G. Mieskes, Y. Moriyama, J. Klingauf, H. Grubmuller, J. Heuser, F. Wieland, R. Jahn, *Cell* **2006**, *127*, 831.

[103] J. Li, W. Wang, X. Zhang, H. Yao, Z. Wei, X. Li, X. Mu, J. Jiang, H. Zhang, *RSC Adv.* **2018**, *8*, 21316.

[104] G. M. Pescador, C. D. Florentsen, H. Østbye, S. L. Sønder, T. L. Boye, E. L. Veje, A. K. Sonne, S. Semsey, J. Nylandsted, R. Daniels, P. M. Bendix, *ACS Nano* **2019**, *13*, 6689.

[105] E. Sezgin, H. J. Kaiser, T. Baumgart, P. Schwille, K. Simons, I. Levental, *Nat. Protoc.* **2012**, *7*, 1042.

[106] E. T. Castellana, P. S. Cremer, *Surf. Sci. Rep.* **2006**, *61*, 429.

[107] J. Andersson, I. Køper, *Membranes* **2016**, *6*, 30.

[108] B. v. Lengerich, R. J. Rawle, P. M. Bendix, S. G. Boxer, *Biophys. J.* **2013**, *105*, 409.

[109] M. Dodes Traian, F. González Flecha, V. Levi, *J. Lipid Res.* **2012**, *53*, 609.

[110] K. K. L. Hoejholt, T. Mužić, S. Jensen, L. Dalgaard, M. Bilgin, J. Nylandsted, T. Heimburg, S. Frandsen, J. Gehl, *Sci. Rep.* **2019**, *9*, 4758.

[111] V. P. Ivanova, T. Heimburg, *Phys. Rev. E* **2001**, *63*, 041914.

[112] B. Wang, L. Zhang, S. C. Bae, S. Granick, *Proc. Natl. Acad. Sci. USA* **2008**, *105*, 18171.

[113] A. Mezni, I. Balti, A. Mlayah, N. Jouini, L. S. Smiri, *J. Phys. Chem. C* **2013**, *117*, 16166.

[114] Q. Jiang, Z. Luo, Y. Men, P. Yang, H. Peng, R. Guo, Y. Tian, Z. Pang, W. Yang, *Biomaterials* **2017**, *143*, 29.

[115] G. T. Yu, L. Rao, H. Wu, L. L. Yang, L. L. Bu, W. W. Deng, L. Wu, X. Nan, W. F. Zhang, X. Z. Zhao, W. Liu, Z. J. Sun, *Adv. Funct. Mater.* **2018**, *28*, 1801389.

[116] C. Liu, W. Zhang, Y. Li, J. Chang, F. Tian, F. Zhao, Y. Ma, J. Sun, *Nano Lett.* **2019**, *19*, 7836.

[117] M. S. Yavuz, Y. Cheng, J. Chen, C. M. Cobley, Q. Zhang, M. Rycenga, J. Xie, C. Kim, K. H. Song, A. G. Schwartz, L. V. Wang, Y. Xia, *Nat. Mater.* **2009**, *8*, 935.

[118] T. Andersen, A. Kyrsting, P. M. Bendix, *Soft Matter* **2014**, *10*, 4268.

[119] P. Urban, S. R. Kirchner, C. Mühlbauer, T. Lohmüller, J. Feldmann, *Sci. Rep.* **2016**, *6*, 22686.

[120] Y. Tang, X. Wang, J. Li, Y. Nie, G. Liao, Y. Yu, C. Li, *ACS Nano* **2019**, *13*, 13015.

[121] C. Corbo, R. Molinaro, F. Taraballi, N. E. Toledano Furman, K. A. Hartman, M. B. Sherman, E. De Rosa, D. K. Kirui, F. Salvatore, E. Tasciotti, *ACS Nano* **2017**, *11*, 3262.

[122] R. Weissleder, *Nat. Biotechnol.* **2001**, *19*, 316.

[123] Y. Liu, P. Maccarini, G. M. Palmer, W. Etienne, Y. Zhao, C. T. Lee, X. Ma, B. A. Inman, T. Vo-Dinh, *Sci. Rep.* **2017**, *7*, 8606.

[124] A. R. Rastinehad, H. Anastos, E. Wajswol, J. S. Winoker, J. P. Sfakianos, S. K. Doppalapudi, M. R. Carrick, C. J. Knauer, B. Taouli, S. C. Lewis, A. K. Tewari, J. A. Schwartz, S. E. Canfield, A. K. George, J. L. West, N. J. Halas, *Proc. Natl. Acad. Sci. USA* **2019**, *116*, 18590.

2000616 (17 of 17)